

## Hyperfine Structure and Nuclear Moments of Lu<sup>175</sup>

GEORGE J. RITTER\*

*Division of Pure Physics, National Research Council, Ottawa, Canada*

(Received November 6, 1961)

The hyperfine structures of the  $5d6s^2\ ^2D_{3/2}$  ground state of Lu<sup>175</sup> and its associated  $^2D_{3/2}$  metastable state have been studied by means of the atomic beam magnetic resonance method. Radio-frequency transitions belonging to seven of the eight hfs intervals have been measured, as well as low-frequency ( $\Delta F=0$ ) transitions at various magnetic fields in both states. The analysis of these data by means of an electronic computer yields not only precise values for the different interaction constants and the electronic  $g$  factors, but also the first directly measured value for the nuclear  $g$  factor of Lu<sup>175</sup>. The results are as follows.  $^2D_{3/2}$ :  $A=194.3316\pm 0.0004$  Mc/sec,  $B=1511.4015\pm 0.0030$  Mc/sec,  $g_I=-0.79921\pm 0.00008$ ,  $g_I' = +(3.50\pm 0.16)\times 10^{-4}$  (with  $\mu_I$  expressed in Bohr magnetons), whence  $\mu_I = +(2.25\pm 0.10)$  nm.  $^2D_{5/2}$ :  $A=146.7790\pm 0.0008$  Mc/sec,  $B=1860.6480\pm 0.0080$  Mc/sec,  $g_I=-1.20040\pm 0.00016$ ,  $g_I'$

$= +(3.13\pm 0.24)\times 10^{-4}$  (with  $\mu_I$  expressed in Bohr magnetons), whence  $\mu_I = +(2.01\pm 0.15)$  nm.

The values for the nuclear magnetic moment quoted for the two states are somewhat different from one another, even though their limits of error just overlap. The reason for this difference is not fully understood. For the present the mean of the two values, viz.  $\mu_I = +(2.17\pm 0.19)$  nm (corrected for diamagnetic shielding effect) is taken as the best value. The nuclear electric quadrupole moment has been calculated from the  $B$  factors to be  $Q = +(5.68\pm 0.06)\times 10^{-24}$  cm<sup>2</sup> (without Sternheimer correction). The accuracy of the present investigation was not sufficient to allow the derivation of an octupole moment.

In the interpretation of the experimentally observed  $A$  factors configuration mixing had to be considered.

### I. INTRODUCTION

THE rare-earth elements ( $Z=58$  to  $71$ ) are of interest both on account of their atomic ground states and on account of their nuclear moments. Optical hyperfine-structure studies indicated that  $^{175}\text{Lu}$  has one of the largest electric quadrupole moments observed so far. It has a nuclear spin  $I = \frac{7}{2}$ .<sup>1</sup> Its electronic ground state is a  $5d6s^2\ ^2D_{3/2}$  state, separated by  $1993.92$  cm<sup>-1</sup> from the  $^2D_{5/2}$  metastable state.<sup>2</sup> The hfs of these states had been studied optically by Gollnow<sup>3</sup> and more recently by Steudel.<sup>4</sup> The values these authors obtained for the magnetic dipole and electric quadrupole interaction constants are summarized in Table I. Hfs constants for other configurations also investigated by them are not shown, but the nuclear moments derived by considering all the data are given in the table. The relations used in the derivations, however, involve rather uncertain assumptions about some of the parameters. A directly measured value for  $\mu_I$  would be desirable to

test the validity of these assumptions. Such a directly measured value is within the scope of the atomic beam method.

The present investigation on the ground-state hfs of Lu<sup>175</sup> (natural abundance 97.4%) by means of the atomic beam magnetic resonance method yields not only more precise values for the different interaction constants but also precise values for the Landé  $g$  factors of the atomic states as well as a direct value for the nuclear  $g$  factor.

### II. APPARATUS

The atomic beam magnetic resonance apparatus and techniques used in this investigation were essentially the same as those described in previous papers by Lew<sup>5</sup> and Wessel and Lew.<sup>6</sup> Some modifications, however, were introduced to facilitate more precise measurements.

#### (a) Ovens

Tubular tantalum ovens (slit dimensions:  $0.025$  to  $0.038$  cm  $\times$   $0.635$  cm) were used for generating the Lu beams. The ovens were heated to about  $1600$ – $1700^\circ\text{C}$  (as measured with an  $0.65\ \mu$  optical pyrometer, uncorrected for emissivity) by the passage of high alternating currents directly through the walls. A charge of about  $0.5$  to  $0.75$  g lasted for about  $10$ – $15$  hr operating time.

Beams of Cs atoms, used for calibrating the  $C$  field and the mass spectrometer, were produced by means of a steel oven at about  $300^\circ\text{C}$ .

#### (b) Ionizers

For the greater part of these experiments the Lu atoms were detected by means of the electron bombardment ionizer.<sup>6</sup> This ionizer was modified to consist of two parts. The entrance slit, ion chamber, filaments, ion extracting electrode, and tungsten grid were all

TABLE I. Some optical data on Lu<sup>175</sup>.

<i>hfs of the <math>^2D</math> ground state.</i>			
State	Interaction constants		Investigator
	$A$ (Mc/sec)	$B$ (Mc/sec)	
$^2D_{3/2}$	$192.3\pm 3.0$	$1500.0\pm 75.0$	Steudel (1958)
$^2D_{5/2}$	$139.0$	$1910.0$	Gollnow (1936)
	$165.0\pm 21.0$	$1590.0\pm 240.0$	Steudel (1958)
<i>Nuclear moments</i>			
	$\mu_I$	$Q$	Investigator
(in nuclear magnetons)	(in $10^{-24}$ cm <sup>2</sup> )		
	$+2.6\pm 0.5$	$+5.9$	Gollnow (1936)
	$+2.0\pm 0.2$	$+5.6\pm 0.6$	Steudel (1958)

\* National Research Laboratories Postdoctorate Fellow, 1958–60.

<sup>1</sup> H. Schüller and T. H. Schmidt, *Z. Physik* **95**, 265 (1935).

<sup>2</sup> P. F. A. Klinkenberg, *Physica* **XXI**, 53 (1955).

<sup>3</sup> H. Gollnow, *Z. Physik* **103**, 443 (1936).

<sup>4</sup> A. Steudel, *Z. Physik* **152**, 599 (1958).

<sup>5</sup> H. Lew, *Phys. Rev.* **91**, 619 (1953).

<sup>6</sup> G. Wessel and H. Lew, *Phys. Rev.* **92**, 641 (1953).

mounted on the same lavite piece and were thus detachable as a unit from the rest of the assembly, which contained the final accelerator plates and the deflector plates, thus making the filaments and grid more easily accessible for replacement. Other changes included V-shaped thoriated tungsten filaments (0.0127-cm diam wire), spring-loaded at the vertex of the V; filament shields at filament potential, shaped in such a way as to produce some focusing effect for the bombarding electrons. Usual operating conditions were: filament currents of about 1.1 to 1.25 amp, electron accelerating potentials of about 105 to 115 v, and total electron currents about 60 to 70 ma. It was also found that for best signal-to-noise ratio, proper alignment of the electron guide field (about 550 to 700 gauss) was most essential. This alignment was done by trial and error.

The whole ionizer assembly was enclosed in a box provided with entrance and exit slits for the beam, and separately pumped. In this way the background noise was reduced by a factor of about 2, provided the ionizer liquid air trap was properly cooled.

The efficiency of this ionizer was estimated to be better than 0.1%. However, this is not an easy estimate to make, since one is comparing the "collection" efficiencies of two actually different systems (tungsten surface-ionization detector grid and electron-bombardment ionizer, respectively, both applied to Cs) at different locations with respect to the first accelerator electrode. Of course, the detection efficiency of the bombardment ionizer could be increased by increasing the electron currents, but, since background noise was often increased more than proportionately because of local outgassing, nothing was gained in doing so.

The signal-to-noise ratios in the resonance experiments with Lu were usually of the order 6/1 to 10/1, with oven temperatures and other operating conditions as mentioned above.

In the last series of experiments on the direct determination of  $g_I$ , a surface ionization detector was constructed with which Lu atoms were detected<sup>7</sup> with an efficiency at least comparable to that of the aforementioned electron-bombardment ionizer, other conditions like oven temperature being the same. It has the advantage, however, that the background noise level was markedly reduced. This was due to it not being "sensitive" to residual gas molecules in the detector chamber, as was the former. Signal-to-noise ratios were usually of the order 20/1.

The design of the surface ionizer was simple, as shown in Fig. 1: The entrance slit was followed by two repeller electrodes, the potentials of which could be varied independently, then by the filament, lying vertically in the beam path, followed by the first accelerator elec-

trode. The repeller and accelerator electrodes were machined from stainless steel. All these, together with the filament supports, were mounted on a lavite piece as a detachable unit, which could be interchanged with a similar unit, described above, for the electron-bombardment ionizer, so that the rest of the ion-accelerator system was the same as in the case of the electron-bombardment ionizer. No other variations of this design were tried.

Efficient ionization was achieved by using a tungsten ribbon, 0.005×0.038 cm and 2.54 cm long, heated to an apparent temperature of about 2000°C (as measured with an optical pyrometer), by a current of about 3.7 amp. Under these operating conditions, there was no noticeable delay in the reevaporation of Lu as ions (cf. Lew<sup>5</sup> on Pr; Ting<sup>8</sup> on La; Sandars and Woodgate<sup>9</sup> on Eu); that is, the detector response followed incidence almost instantaneously and a 10-cps beam chopper worked satisfactorily.

The residual gas pressure in the detector chamber in these experiments was usually of the order  $3 \times 10^{-7}$  mm Hg, as measured on an ionization gauge at the rear of the chamber.

### (c) Other Aspects of Detection

The ions formed in the ionizer were accelerated and focused by a mass spectrometer assembly onto the first dynode of a Cu-Be electron multiplier. The output signal from this was fed into two parallel channels. In the one, after amplification, the signal passed through a scaling circuit and was aurally monitored by means of earphones. The other channel consisted of narrow band amplifiers, RC-tuned to 10 cps, followed by either a vacuum tube voltmeter or a phase-sensitive detector.

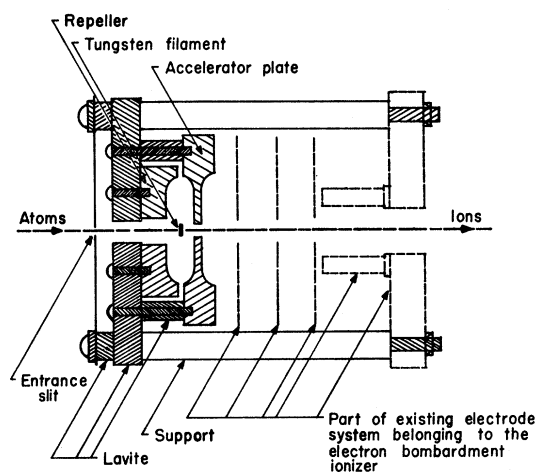


FIG. 1. Schematic diagram of the surface ionization detector used for Lu—looking down the slit lengths.

<sup>7</sup> We are indebted to Dr. I. J. Spalding, formerly of the Cavendish Laboratory, Cambridge, England, now at the Atomic Energy Research Establishment, Harwell, England, for informing us of his successful detection of Lu by means of a tungsten wire.

<sup>8</sup> Y. Ting, Phys. Rev. **108**, 295 (1957).

<sup>9</sup> P. G. H. Sandars and G. K. Woodgate, Proc. Roy. Soc. (London) **A257**, 269 (1960).

The output of this channel was recorded on a 1-ma Westronics strip-chart recorder.

Signal modulation was achieved either by chopping the beam mechanically at 10 cps or else, in the case of field-dependent transitions, by amplitude-modulation of the  $C$  field. The latter was achieved by means of a pair of small Helmholtz coils on Teflon formers sitting next to the rf loop. The current through these coils was interrupted at 10 cps by a motor-driven Tinsley Low Thermal Chopper, type TC-112A. The amplitude of the resulting scanning field was always a few times the resonance linewidths.

This latter method of signal modulation was usually employed; in the last series of experiments, however, beam chopping was used exclusively. In a particular experiment only one of these methods was used for observing both the Lu and the calibrating Cs resonance.

#### (d) Magnets

The  $C$  magnet was changed from the one previously described<sup>5</sup>: new pole pieces (19.05 cm long) were fitted, and, in order to accommodate the field modulation coils mentioned above, the gap was increased to 1.905 cm.

It was found that due to stray fields caused by the  $A$  and  $B$  magnets,  $H_c$  varied considerably over the length of the field. In an attempt to homogenize the  $C$  field and hence reduce the broadening effect on the rf resonances, soft iron shields were placed between the different magnets. This greatly improved the situation and with an rf loop 1.27 cm long, an oven temperature of about 300°C, the Cs low-frequency resonance peaks had widths of about 30 kc/sec, which was of the same order as the "natural" width for the loop under these conditions.

The  $A$  and  $B$  magnets were used with their gradients in the same direction (the "flop-in" arrangement<sup>10</sup>). With the magnet constants given in reference 5, the currents necessary to refocus atoms with equal and opposite effective moments in the two fields were respectively  $i_A \sim 55$  amp and  $i_B \sim 60$  amp.

Because the  $A$  and  $B$  magnets still produced stray field effects in the  $C$  region despite the aforementioned shielding, it was found necessary to regulate the  $A$  and  $B$  currents in order to keep the field in the  $C$  region reasonably constant. The large storage batteries previously used to energize these low-voltage, high-current magnets were therefore supplemented in the course of the investigation by current regulators using power transistors and chopper amplifiers in the manner described by Garwin *et al.*<sup>11</sup> These regulators were capable of giving continuously variable currents up to 100 amp at 6 v with a current regulation of better than one part in  $10^5$ .

A similar regulator was installed for the mass spectrometer magnet, which required 60 amp.

For the  $C$  magnet, a fully charged 2-v 1000-amp-hour battery in series with resistors, specially constructed to eliminate bad contacts, was mostly used; but in the last series of experiments where  $C$  fields of the order 85 gauss and 224 gauss (corresponding to  $i_C \sim 2.6$  amp and 6.0 amp, respectively) were required, the magnet was energized by a current-regulated power supply based on Garwin's first design.<sup>12</sup>

#### (e) rf System and Frequency Measuring Equipment

The frequency-generating and measuring instruments were essentially the same as those used by Ting<sup>8</sup> and Ting and Lew.<sup>13</sup>

The frequency range which had to be covered in order to excite radio-frequency transitions  $\Delta F=0$ ,  $\pm 1$  in the  $^2D$  ground level of Lu<sup>175</sup> extended up to about 2050 Mc/sec. For the low-frequency ( $\Delta F=0$ ) transitions, the following oscillators were used:

- (a) General Radio type 1001A (5 kc/sec—50 Mc/sec);
- (b) A laboratory-built power oscillator (2 Mc/sec—50 Mc/sec).

For the high-frequency ( $\Delta F=\pm 1$ ) transitions, the following were used:

- (a) General Radio type 1208A unit oscillator (65–500 Mc/sec);
- (b) General Radio type 1209A unit oscillator (250–920 Mc/sec);
- (c) General Radio type 1218A unit oscillator (900–2080 Mc/sec);
- (d) Airborne Instruments Lab. oscillator type 124A (300–2500 Mc/sec), with cathode tuning at the lower range and plunger tuning of the external cavity at higher frequencies, for fine frequency control;
- (e) Sylvania 5837 klystron with tunable cavity, immersed in an oil bath (700–2080 Mc/sec).

The filaments of all the latter oscillators were battery operated, thereby increasing the purity of their frequency spectra. Slow-frequency sweep rates were achieved by driving the fine frequency controls with suitably geared-down motor drives.

Frequencies were generally measured by beating against harmonics of a 75-Mc/sec secondary standard in the conventional manner.<sup>8</sup> The beat note between the oscillator frequency and the nearest harmonic of the secondary standard<sup>14</sup> was picked up on a communications receiver and its frequency measured by heterodyning with a General Radio type 620A Hetero-

<sup>10</sup> J. R. Zacharias, Phys. Rev. **61**, 270 (1942).

<sup>11</sup> R. L. Garwin, D. Hutchinson, S. Penman, and G. Shapiro, Rev. Sci. Instr. **30**, 105 (1959).

<sup>12</sup> R. L. Garwin, Rev. Sci. Instr. **29**, 223 (1958).

<sup>13</sup> Y. Ting and H. Lew, Phys. Rev. **105**, 581 (1957).

<sup>14</sup> For correlating the harmonics and the beat notes, suitable absorption wave meters were used.

dyne Frequency Meter. The latter was monitored continuously on a Hewlett-Packard 524B electronic counter, the time base of which was driven by a 100-kc/sec primary standard.

The 75-Mc/sec secondary standard frequency was obtained by multiplication from a crystal-controlled 1-Mc/sec signal, the frequency of which was known to be better than 1 part in 10<sup>8</sup>. Both this 1-Mc/sec signal and the 100-kc/sec primary signal were provided by the Frequency Standards Section of the Division of Applied Physics at this Institute, where it was monitored against the Cs transition frequency in a Cs clock.

In the case of low-frequency transitions, the oscillator frequencies were measured directly on the electronic counter.

### III. RESUME OF THEORY

The hyperfine interaction between the electrons and the nucleus of a free atom in an external magnetic field may be described by the following Hamiltonian<sup>15</sup>:

$$\mathcal{H} = A\mathbf{I}\cdot\mathbf{J} + B \frac{[3(\mathbf{I}\cdot\mathbf{J})^2 + \frac{3}{2}\mathbf{I}\cdot\mathbf{J} - I(I+1)J(J+1)]}{2I(2I-1)J(2J-1)} - g_I\mu_0\mathbf{J}\cdot\mathbf{H} - g_I'\mu_0\mathbf{I}\cdot\mathbf{H} \quad (1)$$

In this expression the first two terms represent, respectively, the energy of interaction between the nuclear magnetic dipole moment and the magnetic field of the electrons at the position of the nucleus, and the energy of interaction between the nuclear electric quadrupole moment and the electric field gradient due to the electrons,  $A$  and  $B$  being the respective interaction constants. The last two terms represent the interaction energy of the magnetic dipole moment of the electrons and of the nucleus, respectively, with the externally applied magnetic field  $\mathbf{H}$ ;  $g_I'$  is the nuclear  $g$  factor [ $\mu_I/(\mu_0I)$ ];  $g_I$  is the electronic  $g$  factor<sup>16</sup> [ $\mu_J/(\mu_0J)$ ];  $\mathbf{I}$  and  $\mathbf{J}$  are the nuclear and electronic angular momenta in units of  $\hbar$ , and  $\mu_0$  is the Bohr magneton.

For an electron with  $L \neq 0$  outside closed shells, the interaction constants  $A$  and  $B$  in the first-order theory have the following explicit forms in terms of the fundamental atomic and nuclear quantities<sup>15,17,18</sup>:

$$A = g_I' \frac{\mu_0^2}{h \times 10^6} \left[ \frac{2L(L+1)}{J(J+1)} \right] F(L, J, Z_i) \left\langle \frac{1}{r^3} \right\rangle_J \text{ Mc/sec}, \quad (2a)$$

<sup>15</sup> See, for example, N. F. Ramsey, *Molecular Beams* (Oxford University Press, New York, 1956) Chap. 3, p. 51.

<sup>16</sup> The sign convention is taken so that the  $g$  factor for the free electron is negative [see, for example, W. A. Nierenberg, *Ann. Rev. Nuclear Sci.* **7**, 349 (1957)]. As indicated above,  $g_I'$  is the ratio of the nuclear magnetic moment in Bohr magnetons to the spin in  $\hbar$ .  $g_I$  (without prime) is thus reserved for its customary usage as the nuclear gyromagnetic ratio when the nuclear magnetic moment is in nuclear magnetons.

<sup>17</sup> H. B. G. Casimir, *On the Interaction between Atomic Nuclei and Electrons* (Teyler's Tweede Genootschap, Haarlem, 1936).

<sup>18</sup> H. Kopfermann, *Nuclear Moments* (English translation, Academic Press Inc., New York, 1958).

and

$$B = \frac{e^2 Q}{h \times 10^6} \left( \frac{2J-1}{2J+2} \right) R(L, J, Z_i) \left\langle \frac{1}{r^3} \right\rangle_J \text{ Mc/sec}, \quad (2b)$$

in which  $F(J, Z_i)$  and  $R(L, J, Z_i)$  are relativistic correction factors given by Casimir<sup>17</sup> and tabulated by Kopfermann.<sup>18</sup> The mean value  $\langle 1/r^3 \rangle$  is usually evaluated from the fine-structure splitting  $\delta$  between the  $(L+\frac{1}{2})$  and  $(L-\frac{1}{2})$  electronic states,<sup>17</sup>

$$\delta = 2.911 H(L, Z_i) Z_i (2L+1) \langle a_0^3/r^3 \rangle \text{ cm}^{-1}, \quad (2c)$$

where  $a_0$  is the Bohr radius;  $Z_i$  is the effective nuclear charge as seen by the electron when inside the atomic core; and  $H(L, Z_i)$  is another relativistic correction factor.

As was shown by Schwartz<sup>19</sup> in a review of the theory of hyperfine structure, the hfs interaction constants in the Hamiltonian (1) might be affected not only by mutual perturbation between neighboring fine-structure levels, but also, much more seriously, by the mixing of higher configurations with the ground configuration, of the sort first discussed by Fermi and Segré.<sup>20</sup>

Considering configurations of the type  $s^2l$  (or  $s^2l^{-1}$ ), Schwartz showed that admixture of a configuration with one of the  $s$  electrons raised to a higher principal quantum number would affect the dipole interaction constant directly and by a considerable amount, whereas the quadrupole interaction constant would be changed only slightly via second-order perturbation of the dipole interaction.<sup>21</sup>

It is possible, however, to correct the constants,  $A$ , for this type of configuration mixing. If they have been measured in both the  $J=L+\frac{1}{2}$  and the  $J=L-\frac{1}{2}$  electronic states, one may write simultaneous expressions of the form  $A = A_0 + \delta(s)$  for both states where  $A$  is the interaction constant evaluated from the experimental data with the aid of the Hamiltonian (1),  $A_0$  is the first-order interaction constant due to the  $d$  electron in the absence of configuration interaction, and  $\delta(s)$  is the contribution<sup>22</sup> due to the  $s$  electrons. Using the theoretical relations between the  $A$ 's and the  $\delta$ 's, given by Schwartz, one may then solve for the unperturbed  $A_0$  of the two states. Denoting these by  $A_0'$  and  $A_0''$  for the  ${}^2D_{\frac{3}{2}}$  and  ${}^2D_{\frac{5}{2}}$  states, respectively, one may write

$$A_0''/A_0' = \theta [J'(J'+1)/J''(J''+1)] \quad (3a)$$

and

$$\delta'(s) = -\delta''(s), \quad (3b)$$

<sup>19</sup> C. Schwartz, *Phys. Rev.* **97**, 380 (1955).

<sup>20</sup> E. Fermi and E. Segré, *Z. Physik* **82**, 729 (1933).

<sup>21</sup> See also: T. G. Eck and P. Kusch, *Phys. Rev.* **106**, 958 (1957).

<sup>22</sup> This  $\delta(s)$  is proportional to Schwartz's  $\Delta_{JJ}$  (see Ting<sup>7</sup>).

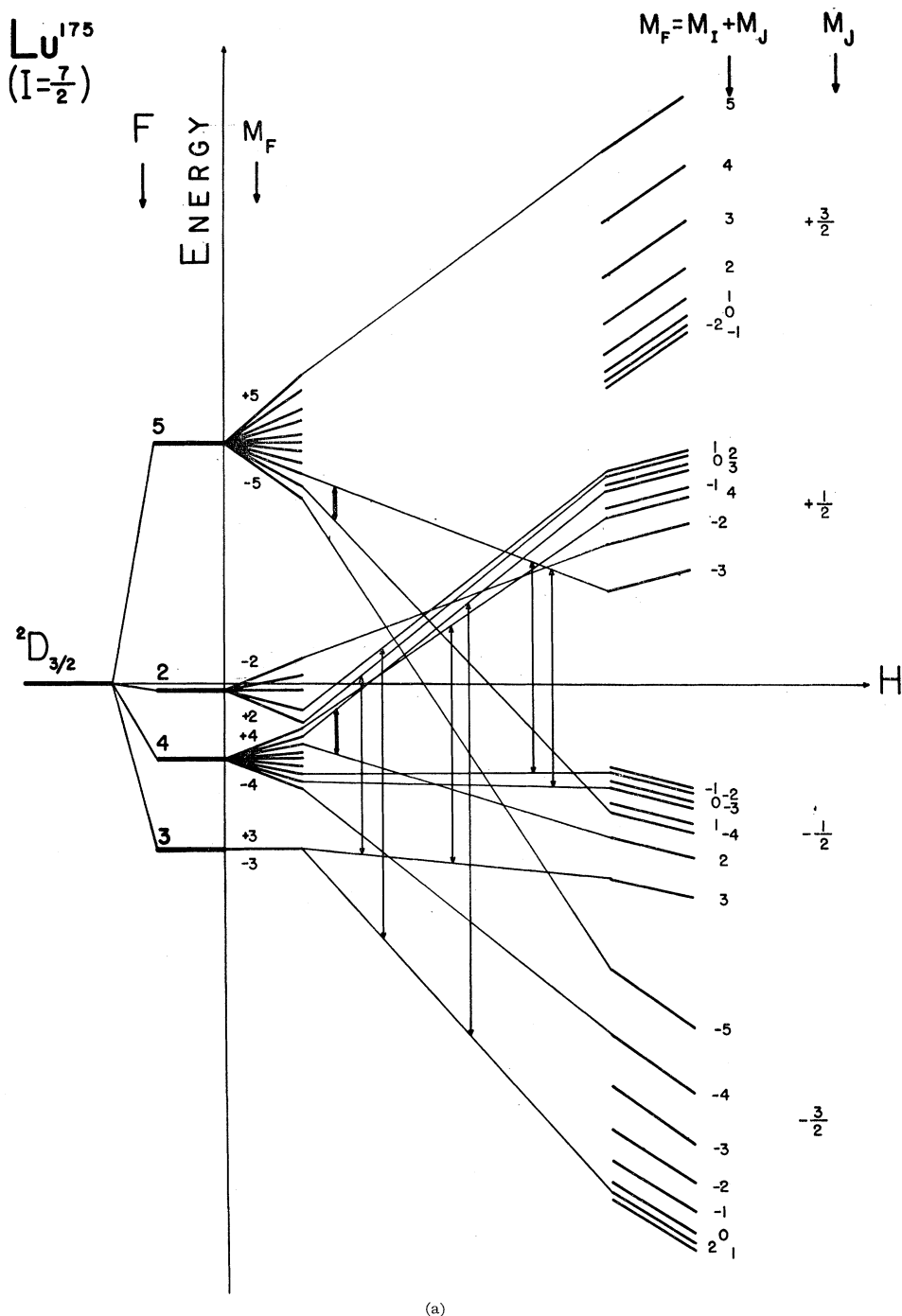


FIG. 2(a). Schematic energy-level diagram of the hfs in the  ${}^2D_{3/2}$  electronic ground state of  $\text{Lu}^{175}$ .

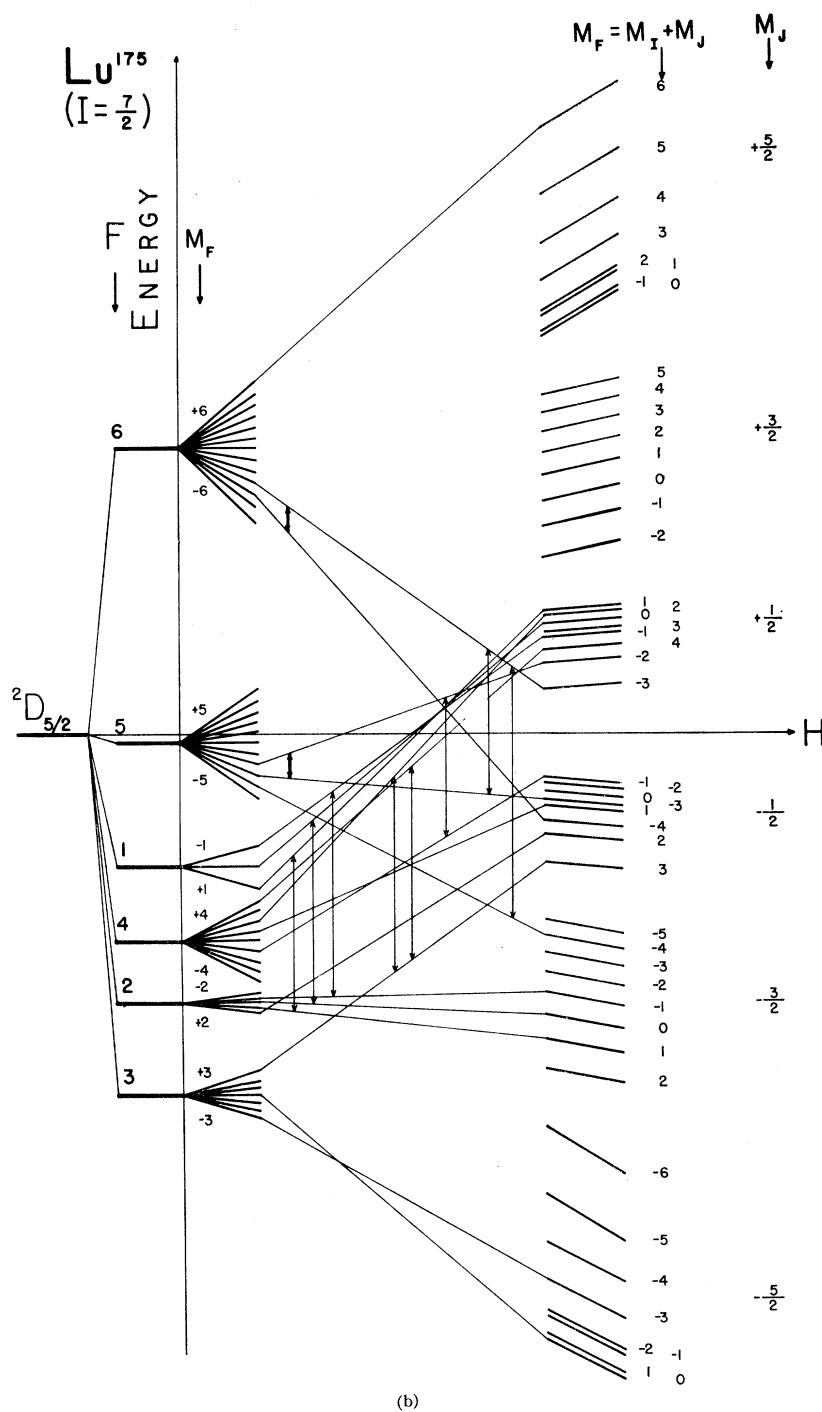
with  $\theta = F''/F'$ ,<sup>23</sup> in which the  $F$ 's are the correction factors introduced above.

<sup>23</sup> Strictly speaking  $\theta = (F''/F')|C''/C'|^2$ , where the  $C$ 's are normalization constants, close to unity, which give the density at the nucleus of the wave functions for the valence electron in each of the two states (see references 17, 19). In expression (2a) they are contained in the factor  $[(1/r^3)]_r$ . Casimir<sup>17</sup> has given a formula by means of which the ratio  $|C''/C'|^2$  can be calculated. This formula is apparently fairly reliable for the lighter elements ( $Z \leq 50$ ) where these constants are not very large anyway, but

The energy levels of an atom may be obtained by solving the secular equation derived from the Hamiltonian (1). In very weak and very strong magnetic fields, perturbation methods are adequate if the representation is suitably chosen. In intermediate fields, however, the secular equation has to be solved numerically.

for the heavier elements it should be used with caution. For lack of better information,  $|C''/C'| = 1$  is therefore assumed for all cases in the present work.

FIG. 2(b). Schematic energy-level diagram of the hfs in the  $^2D_{5/2}$  electronic state of Lu<sup>175</sup>.



In the absence of an external magnetic field, the  $^2D_{5/2}$  ground state of Lu<sup>175</sup> consists of four hfs levels labeled by  $F=5, 4, 3,$  and  $2$ . They are not in their normal sequence, as shown schematically in Fig. 2(a), since the electric quadrupole interaction is large compared to the magnetic dipole interaction. This pattern was first deduced by Steudel<sup>4</sup> by interferometric methods. It has been confirmed by the present more accurate measurements.

The zero field hfs pattern of the  $^2D_{5/2}$  metastable state consists of 6 levels with  $F=6, 5, 4, 3, 2,$  and  $1$ . In this case, previous optical work<sup>3,4</sup> still left doubt as to the exact pattern, since the close-lying levels could not be resolved. The present measurements indicate a pattern as shown in Fig. 2(b).

In a weak external magnetic field the degeneracy of the hfs levels is removed and each  $F$  level splits into a number of magnetic substates denoted by the quantum

number  $m_F$ . This is true for all the levels studied here, except for the level  $F=3$  in the  ${}^2D_{3/2}$  state which remains degenerate for low values of  $H_c$ —only at higher  $H_c$  values does it lose its degeneracy, in which case the  ${}^2D_{3/2}$  ground state then splits into 32 magnetic substates. The  ${}^2D_{3/2}$  level splits into 48 magnetic states. These weak-field energy levels are shown schematically in Fig. 2, together with the strong-field quantum numbers,  $m_J$  and  $m = m_L + m_J$ .

Magnetic dipole transitions between the different magnetic substates at weak fields are governed by the selection rules  $\Delta F=0, \pm 1$ ;  $\Delta m_F = \pm 1$  ( $\pi$  transitions) and  $\Delta F = \pm 1, \Delta m_F = 0$  ( $\sigma$  transitions). However, for a transition to be observable in a “flop-in” experiment such as in this case, there is an extra condition that has to be fulfilled, namely, that  $m_J$  must change its sign when such a transition occurs. This latter requirement simplifies the spectrum considerably without reducing the amount of useful information obtainable.

The transitions measured accurately in the present investigation are indicated by arrows in Fig. 2.

#### IV. MEASUREMENTS AND DATA

Two series of measurements were made. The aim of the first series was to obtain accurate values for the interaction constants,  $A$  and  $B$ , of the  ${}^2D_{3/2}$  and  ${}^2D_{5/2}$  states, as well as for their electronic  $g$  factors. In the second series of experiments, selected transitions were measured as precisely as possible in an attempt to extract a value for  $g_I'$  directly.

##### (a) Hyperfine Structure Intervals and $g_J$

Lines belonging to all seven of the intervals which were observable in the present experimental arrangement were measured; transitions belonging to the  $F=2 \leftrightarrow 3$  interval in the  ${}^2D_{3/2}$  state were not observable because  $m_J$  does not change sign. Not all the observed Zeeman lines were measured to the same degree of accuracy. In each hfs interval, however, at least two different transitions (different magnetic substates) were measured accurately and with care. For example, in the case of the  ${}^2D_{3/2}(2 \leftrightarrow 3)$  interval several transitions were observed, but only the  $[(2;2) \leftrightarrow (3;1,3)]$  and  $[(2;1) \leftrightarrow (3;0,2)]$  transitions were measured with accuracy. Still, the less accurately measured transitions were of value when locating an interval. On the average, for each transition the frequencies were measured at about 5 or 6 different values of  $H_c$ , ranging from about 0.65 gauss to 3.0 gauss.

Low-frequency ( $\Delta F=0$ ) transitions were observed in the  $F=5$  and  $F=4$  levels of the  ${}^2D_{3/2}$  state and in the  $F=6, 5$ , and 4 levels of the  ${}^2D_{5/2}$  state. The ones indicated by double-barred arrows in Fig. 2 were measured accurately for the evaluation of the  $g$  factors.

The magnitude of the  $C$  field,  $H_c$ , was evaluated by means of the low-frequency Cs transition,  $[(4, -3) \leftrightarrow (4, -4)]$ . In the case of  $\sigma$  transitions for Lu,  $\nu_{Cs}$  at

the position of the  $\sigma$  loop was obtained by interpolation. On each side of the  $\sigma$  loop, at equal distances, about 4.45 cm away, were  $\pi$  loops. The Cs frequencies at their positions were obtained and the average of these were then taken as the resonance value at the  $\sigma$  loop.

With the rf loops used (1.27-cm  $\pi$  loops and 2.54-cm  $\sigma$  loop) the Lu peaks had widths ranging from 30 to 160 kc/sec, depending on the field dependence of the transition under consideration. The Cs peaks usually had widths of the order 30 kc/sec.

The resonances which were observed for the  ${}^2D_{3/2}(6, -3) \leftrightarrow (5, -3)$  transition using the above-mentioned  $\sigma$  loop, were double-peaked. None of the other Lu resonances showed this line shape, though similar effects were observed with the same rf loop for resonances in the ground state of  $\text{Na}^{23}$  which occurred in the same frequency region. These double-peaked structures could be ascribed to a variation in rf amplitude over the length of the loop (see Ramsey<sup>24</sup> and also Woodgate and Hellwarth<sup>25</sup>) in this particular frequency region. The frequency of the dip between the two peaks was taken as the resonance frequency. The frequencies thus obtained, were consistent with those of the  $(6, -3) \leftrightarrow (5, -4)$  transition, taken with a  $\pi$  loop.

For each nominal value of  $H_c$  usually 6 to 9 peaks of a kind were recorded on the strip-chart recorder, when the rf was changed slowly through resonance at constant field. The lines were swept backwards and forwards to average out the effect of the finite time constant of the detection and recording equipment.

As mentioned previously, in the earlier measurements the  $C$  field was unregulated, hence as the batteries discharged the  $C$  field used to drift with time, usually at a constant rate over a single run. The procedure was therefore to alternate sequences of three (say) Lu peaks with sequences of three Cs peaks. The resulting drift of Lu peaks with time used to follow that of Cs in the proper relation. In such cases the experimentally observed frequencies were plotted against time and the values for  $\nu_{Cs}$  and  $\nu_{Lu}$  at any given time could then be read off the same graph. Such values were then used in the computations.

In this way the large number of runs resulted in altogether twenty-two  $\Delta F=0$  and fifty  $\Delta F = \pm 1$  resonance frequencies in the  ${}^2D_{3/2}$  state, and thirteen  $\Delta F=0$  and thirty-five  $\Delta F = \pm 1$  in the  ${}^2D_{5/2}$  state, with a corresponding number of Cs frequencies.

In assigning limits of error to these values, several factors were taken into consideration: number of peaks for a particular run and their scatter; signal-to-noise ratio, shape and width of the peaks; rate of drift of the  $C$  field and the closeness with which the Lu peaks followed. Of these factors, the first mentioned was usually regarded of greatest importance; where a large number of peaks were available in a given run, usually more than

<sup>24</sup> N. F. Ramsey, Phys. Rev. **76**, 996 (1949).

<sup>25</sup> G. K. Woodgate and R. W. Hellwarth, Proc. Phys. Soc. (London) **A69**, 588 (1956).

70% of them fell within the assigned limits. Where only a few peaks were available, the stated errors embrace the entire scatter.

Depending on the frequency range, the accuracy of the  $\Delta F = \pm 1$  transition frequencies in the  $^2D_{3/2}$  state was mostly of the order 1 part in  $10^5$  to 1 part in  $10^6$ , while in the  $^2D_{5/2}$  state the values were slightly less accurate, partly because of lower peak intensities. They ranged from 1 part in  $10^4$  to 2 parts in  $10^6$ .

In Table II, a typical set of experimental data obtained in the way described above is given. These data are for the transitions  $[(4,3) \leftrightarrow (3,2)]$  and  $[(4,4) \leftrightarrow (3,3)]$  in the  $^2D_{3/2}$  state, together with the different calibrating Cs frequencies.

### (b) Determination of $g_I'$

Attempts were made to obtain the nuclear gyromagnetic ratio,  $g_I'$ , and hence  $\mu_I$ , of Lu<sup>175</sup> directly by means of conventional NMR techniques in bulk matter. These attempts were unsuccessful at first, probably due to strong relaxation effects, caused by the interaction of the exceptionally large electric-quadrupole moment of the Lu nuclei with their surroundings, in the compounds examined. It is, however, possible to obtain  $g_I'$  directly from atomic beam studies of hfs.<sup>26,27</sup> Appropriate measurements were therefore made for such a determination. Since completion of these measurements, the previous search of Lu NMR in bulk matter has been resumed. These attempts have finally been successful; the magnetic resonance peak due to the Lu nuclei has been observed when the latter were embedded in a suitably symmetric lattice.<sup>28</sup> The preliminary results confirm the values obtained from the atomic beam measurements described below.

In the Hamiltonian (1) the nuclear magnetic moment enters not only through the term  $A\mathbf{I} \cdot \mathbf{J}$  but also through the term  $g_I' \mu_0 \mathbf{I} \cdot \mathbf{H}$ . This term, however, is much smaller than the term  $g_J \mu_0 \mathbf{J} \cdot \mathbf{H}$  and in most atomic beam measurements even at moderately high fields, it is difficult to extract an accurate value for  $g_I'$  from the resonance data. One of the reasons for this is that, as one goes to higher fields to make the  $g_I'$  term as large as possible, inhomogeneities in the  $C$  field broaden the lines so much that the relative accuracy is not improved. It so happens, however, that certain of the observable lines in the  $^2D_{3/2}$  and  $^2D_{5/2}$  states of Lu go through a point of zero field dependence at reasonably high fields. At such points the lines are narrower than elsewhere and hence can be measured to a higher precision than at field-dependent points. One such line is the  $[(2,2) \leftrightarrow (3,3)]$  line in the  $^2D_{3/2}$  state which goes through a minimum at about 85 gauss; another is the  $[(4, -1) \leftrightarrow (5, -2)]$  line of the

TABLE II. Typical set of experimental data for the transitions  $[(4,3) \leftrightarrow (3,2)]$  and  $[(4,4) \leftrightarrow (3,3)]$  in the  $^2D_{3/2}$  state, together with the calibrating Cs frequencies.

$\nu_{Cs}$ (Mc/sec)	(a) $\nu_{Lu}[(4,3) \leftrightarrow (3,2)]$ (Mc/sec)
0.3025±0.0015	346.0848±0.0030
0.3103±0.0020	346.0904±0.0050
0.5949±0.0010	346.6526±0.0020
0.5957±0.0015	346.6530±0.0025
0.7655±0.0020	346.9900±0.0020
0.7836±0.0015	347.0284±0.0020
0.9967±0.0015	347.4510±0.0030
0.9996±0.0010	347.4562±0.0020
$\nu_{Cs}$ (Mc/sec)	(b) $\nu_{Lu}[(4,4) \leftrightarrow (3,3)]$ (Mc/sec)
0.3008±0.0020	346.2706±0.0020
0.3334±0.0020	346.3538±0.0035
0.5881±0.0015	347.0048±0.0035
0.6016±0.0015	347.0344±0.0030
0.7991±0.0015	347.5462±0.0030
0.8016±0.0015	347.5560±0.0025
1.0006±0.0015	348.0664±0.0015
1.0020±0.0015	348.0714±0.0015
1.0062±0.0020	348.0764±0.0030

$^2D_{3/2}$  state which goes through a minimum at about 224 gauss. These two lines have accordingly been measured with greater relative precision than those in the first series of experiments described in the previous paragraphs.

It should be pointed out that, in general, one cannot obtain an explicit expression for the frequency of a transition at intermediate fields. The secular equations are usually of higher degree than the second. Numerical methods must then be used. This is true also for the two lines mentioned above. The task of extracting a value for  $g_I'$  from the measurements would thus be extremely tedious were it not for the fact that electronic computer programs for calculations of this type are available.<sup>29-31</sup>

In Table III the resonance frequencies of the two transitions are given for the relevant regions. In Fig. 3 the observed frequencies for the  $^2D_{3/2}[(2,2) \leftrightarrow (3,3)]$  transitions, are plotted as a function of  $\nu_{Cs}$ , i.e., of  $H_c$ .

The resonance peaks were indeed very much narrower in the regions of zero field dependence. For a 3.8-cm  $\pi$  loop, the half-intensity widths were about 10 to 15 kc/sec, i.e., about 3 to 4 times smaller than in the field-dependent region. For measurements on the  $[(2,2) \leftrightarrow (3,3)]$  transition, both such a 3.8-cm  $\pi$  loop and a 1.27-cm loop were used, while for the  $[(4, -1) \leftrightarrow (5, -2)]$  transition in the  $^2D_{3/2}$  state only the 1.27-cm loop was used. This, together with the fact that the  $^2D_{3/2}$  resonances were slightly weaker than those belonging to the  $^2D_{5/2}$

<sup>26</sup> See, for example, H. L. Garvin, T. M. Green, E. Lipworth, and W. A. Nierenberg, Phys. Rev. **116**, 393 (1959).

<sup>27</sup> For other methods see, for example, J. Eisinger, B. Bederson, and B. T. Feld, Phys. Rev. **86**, 73 (1952); G. K. Woodgate and P. G. H. Sandars, Nature **181**, 1395 (1958).

<sup>28</sup> A. H. Reddoch and G. J. Ritter (to be published).

<sup>29</sup> W. A. Nierenberg, University of California Radiation Laboratory Report UCRL-3816, 1957 (unpublished).

<sup>30</sup> L. L. Marino, thesis, University of California Radiation Laboratory, UCRL-8721, 1959 (unpublished).

<sup>31</sup> V. J. Ehlers, thesis, University of California Radiation Laboratory, UCRL-9123, 1960 (unpublished).



TABLE III. Observed resonance frequencies for the  ${}^2D_{3/2}[(2,2) \leftrightarrow (3,3)]$  and  ${}^2D_{3/2}[(4,-1) \leftrightarrow (5,-2)]$  transitions in the region of zero field dependence.

${}^2D_{3/2}[(2,2) \leftrightarrow (3,3)]$	
$\nu_{Cs}[(4,-3) \leftrightarrow (4,-4)]$ (Mc/sec)	$\nu_{Lu}[(2,2) \leftrightarrow (3,3)]$ (Mc/sec)
28.5060±0.0100	430.2920±0.0150
28.5830±0.0100	430.2500±0.0100
29.3785±0.0040	429.8544±0.0050
29.3795±0.0040	429.8560±0.0050
29.6440±0.0080	429.7744±0.0040
29.6527±0.0060	429.7720±0.0040
29.7360±0.0150	429.7460±0.0100
29.7622±0.0040	429.7470±0.0050
30.0825±0.0075	429.6970±0.0015
30.2710±0.0050	429.6828±0.0010
30.2800±0.0050	429.6824±0.0010
30.4970±0.0100	429.6860±0.0100
30.5130±0.0035	429.6874±0.0030
30.5267±0.0035	429.6900±0.0030
30.5900±0.0025	429.6954±0.0035
30.8630±0.0100	429.7340±0.0100
30.8950±0.0100	429.7420±0.0150
30.9170±0.0050	429.7446±0.0030
31.2300±0.0050	429.8390±0.0040
31.2297±0.0025	429.8384±0.0025
31.2520±0.0030	429.8490±0.0025
31.2577±0.0075	429.8470±0.0040
31.2597±0.0060	429.8480±0.0025
32.5300±0.0040	430.6400±0.0050
32.6020±0.0050	430.7080±0.0080
32.6020±0.0025	430.6980±0.0050
32.6175±0.0025	430.7120±0.0050

${}^2D_{3/2}[(4,-1) \leftrightarrow (5,-2)]$	
$\nu_{Cs}[(4,-3) \leftrightarrow (4,-4)]$ (Mc/sec)	$\nu_{Lu}[(4,-1) \leftrightarrow (5,-2)]$ (Mc/sec)
76.7856±0.0250	395.9498±0.0180
79.3804±0.0300	394.2024±0.0080
81.0019±0.0150	393.5595±0.0075
81.7183±0.0250	393.3861±0.0080
82.4746±0.0150	393.2706±0.0075
82.8790±0.0075	393.2335±0.0025
82.8860±0.0075	393.2330±0.0025
83.0810±0.0250	393.2283±0.0050
83.2759±0.0200	393.2234±0.0050
83.9471±0.0350	393.2500±0.0030
84.0230±0.0100	393.2645±0.0050
84.2515±0.0100	393.2816±0.0075
84.3430±0.0150	393.3015±0.0035
84.9743±0.0300	393.4181±0.0060
85.9120±0.0400	393.7032±0.0075
87.7768±0.0250	394.6086±0.0100
89.0035±0.0350	395.3894±0.0180

state, is part of the reason why larger limits of error were assigned in the former case.

The ultimate accuracy in both cases was limited by instabilities in the  $C$  field, observed both with and without the magnet current regulated. These instabilities reduced the accuracy with which particularly  $\nu_{Cs}$  could be obtained. It would therefore be advisable to control the  $C$  field itself, rather than just the magnet current, before a more accurate determination of  $g_I'$  is attempted. This will be done in a future project.

## V. EVALUATION OF $A$ , $B$ , $g_J$ , AND $g_I'$ . DISCUSSION

### (a) Preliminary Results

The first estimates of the interaction constants  $A$  and  $B$  for the two states were obtained from the experi-

mental data by means of perturbation calculations combined with graphical methods. The results are given in Table IV. The  $g_J$  values, also given in the table, were obtained by least-squares fitting of second- and third-order expressions in  $H$  to some of the  $\Delta F=0$  data in each case.  $g_J$  was then extracted from the first-order perturbation coefficients of these expressions.

### (b) Final Evaluation

In order to extract the maximum amount of information with the highest accuracy from the experimental data, these were analyzed on an IBM computer.<sup>32</sup> The computer had been programmed to fit the observed resonance data at all fields to exact numerical solutions of the Hamiltonian (1) and to yield values for  $A$ ,  $B$ ,  $g_J$  and  $g_I'$ .<sup>27</sup> Errors on these quantities were assigned from least-squares considerations.

The accuracy of the present measurements was not considered sufficient to allow a derivation of an octupole interaction constant.

The final results as obtained by utilizing all the accurately measured resonance frequencies in the above-mentioned computer routine, are given in Table V. The fundamental constants used in these calculations were

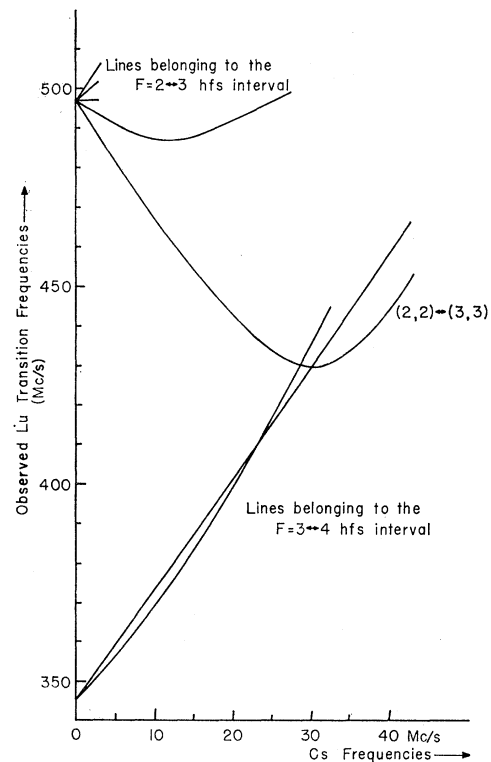


FIG. 3. The experimentally observed variation of the resonance frequencies of some transitions in the  ${}^2D_{3/2}$  ground state of  $\text{Lu}^{175}$  as a function of the calibrating Cs frequencies.

<sup>32</sup> Performed at the University of California, Berkeley, through the courtesy of Dr. Howard A. Shugart.

TABLE IV. Preliminary values for the zero-field hfs intervals,  $A$  and  $B$  (in Mc/sec) and  $g_J$  for the  ${}^2D_{3/2}$  and  ${}^2D_{5/2}$  states.

${}^2D_{3/2}$	$\Delta\nu(5 \leftrightarrow 4) =$	$2051.229 \pm 0.025$
	$\Delta\nu(4 \leftrightarrow 3) =$	$345.508 \pm 0.015$
	$\Delta\nu(3 \leftrightarrow 2) =$	$-496.560 \pm 0.015$
	$A =$	$194.333 \pm 0.005$
	$B =$	$1511.386 \pm 0.025$
	$g_J =$	$-0.799 \pm 0.001$
${}^2D_{5/2}$	$\Delta\nu(6 \leftrightarrow 5) =$	$1837.588 \pm 0.025$
	$\Delta\nu(5 \leftrightarrow 4) =$	$800.370 \pm 0.025$
	$\Delta\nu(4 \leftrightarrow 3) =$	$161.810 \pm 0.050$
	$\Delta\nu(3 \leftrightarrow 2) =$	not observed
	$\Delta\nu(2 \leftrightarrow 1) =$	$-238.055 \pm 0.003$
	$A =$	$146.789 \pm 0.020$
	$B =$	$1860.608 \pm 0.100$
	$g_J =$	$-1.202 \pm 0.002$

taken from Cohen, Crowe, and Du Mond<sup>33</sup>; the calibrating Cs data from Ramsey.<sup>15</sup>

With these values for  $A$  and  $B$  the zero-field hfs separations are therefore as given below, with a level ordering as already shown in Fig. 2.

${}^2D_{3/2}$

$$\begin{aligned} \Delta\nu_{5 \leftrightarrow 4} &= 5A + (5/7)B = 2051.2305 \pm 0.0040 \text{ Mc/sec,} \\ \Delta\nu_{4 \leftrightarrow 3} &= 4A - (2/7)B = 345.4974 \pm 0.0024 \text{ Mc/sec,} \\ \Delta\nu_{3 \leftrightarrow 2} &= 3A - (5/7)B = -496.5777 \pm 0.0008 \text{ Mc/sec.} \end{aligned}$$

${}^2D_{5/2}$ :

$$\begin{aligned} \Delta\nu_{6 \leftrightarrow 5} &= 6A + (18/35)B = 1837.5792 \pm 0.0100 \text{ Mc/sec,} \\ \Delta\nu_{5 \leftrightarrow 4} &= 5A + (1/28)B = 800.3467 \pm 0.0043 \text{ Mc/sec,} \\ \Delta\nu_{4 \leftrightarrow 3} &= 4A - (8/35)B = 161.8248 \pm 0.0056 \text{ Mc/sec,} \\ \Delta\nu_{3 \leftrightarrow 2} &= 3A - (9/28)B = -157.7283 \pm 0.0051 \text{ Mc/sec,} \\ \Delta\nu_{2 \leftrightarrow 1} &= 2A - (8/28)B = -238.0556 \pm 0.0040 \text{ Mc/sec.} \end{aligned}$$

### (c) Ratios of the Interaction Constants

It has been pointed out in Sec. III that from theoretical considerations (Schwartz<sup>19</sup>) one would expect the ratio of the  $A$  factors in the two components of the  ${}^2D$  level to be

$$A''/A' = (7/3)(F''/F')$$

and the ratio of the  $B$  factors to be

$$B''/B' = (7/10)(R''/R').$$

Assuming  $Z_i \approx 57.8$  [see Sec. VI (b)] and using the appropriate values for the relativistic correction factors,<sup>17,18</sup> these theoretical ratios are

$$A''/A' = 2.4306$$

and

$$B''/B' = 0.7976.$$

From the experimental results, however, it is found that

$$A''/A' = 1.32397 \pm 0.00001$$

<sup>33</sup> E. R. Cohen, K. M. Crowe, and J. W. M. Du Mond, *Fundamental Constants of Physics* (Interscience Publishers, Inc., New York, 1957).

and

$$B''/B' = 0.812298 \pm 0.000005.$$

The large deviation from the theoretically expected ratios, especially for the ratio of the  $A$  factors, points to considerable perturbations of the two  ${}^2D$  terms. These may be caused by mixing with higher electronic configurations, as discussed by Schwartz<sup>19</sup> and mentioned in Sec. III. Similar effects have already been observed in the  ${}^2D$  ground states of La,<sup>8</sup> Y,<sup>34</sup> and Sc,<sup>35</sup> as well as in the HfII spectrum.<sup>36</sup> Furthermore, the fact that configuration interaction of some sort does take place, is borne out by the observation that the isotope shifts in spectral lines belonging to  $5d6d^2$ - $5d6s6p$  transitions for Lu<sup>175</sup> and Lu<sup>176</sup> are not the same, as one would have expected.<sup>4</sup> Electronic configurations that meet the requirements for a configuration interaction of this type in the case of Lu are either the  $5d^26s$  or  $5d6s7s$  configurations, with the former being more likely on account of its lower energy.<sup>2</sup> Even though the percentage mixing might be small, the effect might be considerable, because  $s$  electrons contribute more strongly to the hyperfine energy than the  $d$  electron.

Second-order perturbations among the fine-structure levels,  $J = \frac{3}{2}$  and  $\frac{5}{2}$ , themselves, can also take place. It can be shown, however, that in the present case this particular effect is negligible.

Schwartz<sup>19</sup> has shown how one can correct for configuration mixing in the case where one of the  $s$  electrons is raised to a higher  $s$  state. Applying expressions (3a) and (3b) to the experimental values for  $A''$  and  $A'$ , the corrected values  $A_0'' = 241.679$  Mc/sec and  $A_0' = 99.432$  Mc/sec are obtained. These are the values to be used in the calculations of the nuclear moments.

Configuration mixing may also be responsible for the discrepancy between the observed ratio of the electric quadrupole interaction constants and the theoretically expected. The  $5d6s^2$   ${}^2D$  levels may be perturbed by the  $5d^26s$   ${}^2D$  levels as well as by  $5d6s7s$ . Such a perturbation has been suggested by Murakawa for the similar case of La.<sup>37</sup> Since the effect is relatively small compared to other uncertainties, no attempt is made for the present to correct the  $B$  factors.

 TABLE V. Final  $A$ ,  $B$ ,  $g_I'$ , and  $g_J$  values for the  ${}^2D_{3/2}$  and  ${}^2D_{5/2}$  states.

Quantity \ State	${}^2D_{3/2}$	${}^2D_{5/2}$
$A$ (Mc/sec)	$194.3316 \pm 0.0004$	$146.7790 \pm 0.0008$
$B$ (Mc/sec)	$1511.4015 \pm 0.0030$	$1860.6480 \pm 0.0080$
$g_I'$	$+(3.50 \pm 0.16) \times 10^{-4}$	$+(3.13 \pm 0.24)$
$g_J$	$-(0.79921 \pm 0.00008)$	$-(1.20040 \pm 0.00016)$

<sup>34</sup> G. Fricke, H. Kopfermann, and S. Penselin, *Z. Physik* **154** 218 (1959).

<sup>35</sup> G. Fricke, H. Kopfermann, S. Penselin, and K. Schlüpmann, *Z. Physik* **156**, 416 (1959).

<sup>36</sup> E. Finckh and A. Stuedel, *Z. Physik* **141**, 19 (1955).

<sup>37</sup> K. Murakawa, *Phys. Rev.* **110**, 393 (1958).

(d) **Electronic  $g$  factors,  $g_J$** 

The effect of configuration mixing should in general also be detectable in the values of the electronic  $g$  factors of the two fine-structure states. These effects, however, might be quite small, hence, very accurate measurements are necessary.

In Table VI the experimentally observed  $g_J$  values for the  ${}^2D_{3/2}$  and  ${}^2D_{5/2}$  states of Lu are listed together with those observed by Penselin for the same states in yttrium.<sup>38</sup> The theoretically computed values, assuming Russell-Saunders coupling and taking into account the anomalous moment of the electron, are also given.

The good agreement between experiment and theory suggests that if perturbations are taking place, then the perturbing terms must be terms with  $g_J$  factors the same as for the perturbed, since mixing of such terms is known to have a large effect on the  $A$  values but none on the  $g_J$  values. It is therefore possible from these measurements to decide which are the perturbing terms, since in any case, only terms with the same  $J$  and the same parity can perturb each other, and in Russell-Saunders coupling  $g_J=0.8$  and  $1.2$  for  $J=\frac{3}{2}$  and  $\frac{5}{2}$  appear only in  ${}^2D$  terms (apart from  ${}^{10}H$  terms, which are hardly likely in this case). As already mentioned, one such configuration which meets these requirements is the  $5d6s7s$  configuration.

(e) **Nuclear  $g$  Factor,  $g_I'$** 

As shown in Table V the values of  $g_I'$  obtained from measurements in the two fine-structure states are somewhat different from one another even though their limits of error just overlap. On the basis of present atomic theory the two values should be the same, if allowances are made for screening effects of inner electrons. The reason for the difference is not fully understood.

The frequencies calculated for the  $[(4, -1) \leftrightarrow (5, -2)]$  transition in the  ${}^2D_{3/2}$  state by the computer routine on the assumption of  $g_I' = +(3.13 \times 10^{-4})$  are mostly within the uncertainties placed on the experimentally observed data. In the case of the  ${}^2D_{3/2}[(2, 2) \leftrightarrow (3, 3)]$  transition, the calculated frequencies are all well within the experimental uncertainties if  $g_I' = +(3.50 \times 10^{-4})$  is assumed. Hence, both values seem to be valid. However, the possibility of systematic errors in taking Lu and Cs resonance frequencies cannot be completely excluded. Thus, for instance, to see if there was any indication that the transitions were not taking

TABLE VI.  $g_J$  factors for the  ${}^2D_{3/2}$  and  ${}^2D_{5/2}$  electronic states.

	${}^2D_{3/2}$	${}^2D_{5/2}$
Lu	$-0.79921 \pm 0.00008$	$-1.20040 \pm 0.00016$
Y	$-0.79927 \pm 0.00010$	$-1.20028 \pm 0.00017$
Theory	$-0.799542 \pm 0.000006$	$-1.200458 \pm 0.000005$

<sup>38</sup> S. Penselin, Z. Physik **154**, 231 (1959).

place within the confines of the rf loop, the data from loops of different length (1.27 cm and 3.81 cm) were examined critically. No such indication was found. No other source of systematic error has suggested itself. Even so, before deciding whether or not the difference is real, further experiments are necessary.

For the present, the best value for  $g_I'$  is the weighted mean of the two measurements. This is

$$g_I' = +(3.35 \pm 0.29) \times 10^{-4},$$

whence

$$\begin{aligned} \mu_I(\text{uncorrected}) &= g_I' \times 1836.12 \\ &= +2.15 \pm 0.19 \text{ nm} \end{aligned}$$

To correct for the diamagnetic shielding effect of the electrons this value has to be divided by  $(1-\sigma)$ , where  $\sigma=0.0082$  for  $Z=71$ .<sup>15</sup> The corrected value for the nuclear magnetic moment of Lu<sup>175</sup> is therefore

$$\mu_I(\text{Lu}^{175}) = +2.17 \pm 0.19 \text{ nm}$$

It should be emphasized that this value has been obtained without the use of a Fermi-Segré type of formula. It therefore does not suffer from the uncertainties inherent in a determination of the latter type, as discussed in the next section. This value is in reasonably good agreement with the preliminary value of  $2.229 \pm 0.010$  nm obtained by NMR techniques.<sup>28</sup>

VI. DERIVATION OF NUCLEAR MOMENTS FROM  $A, B$ 

With the existence of a fairly accurate NMR value for the nuclear magnetic moment, or even the value 2.17 nm of this experiment, the uncertainties inherent in the use of relations of the type (2a) and (2b) for the calculation of nuclear moments may now be illustrated. These two relations involve the quantity  $\langle 1/r^3 \rangle$ , which is usually evaluated from the fine structure splitting,  $\delta$ , by means of Eq. (2c). However, in order to do so, an estimate of  $Z_i$ , the effective nuclear charge as seen by the electron when inside the atomic core, is needed.

(a) **Effective Nuclear Charge,  $Z_i$** 

In the past, following Casimir,<sup>17</sup> the screening correction,  $\sigma_d$ , for a  $d$  electron in the expression  $Z_i = Z - \sigma_d$ , has been taken empirically as  $\sigma_d \approx 11$  for all  $d$  electrons.<sup>18</sup> This assumption has no sound experimental basis, as was pointed out by Murakawa.<sup>39</sup> He investigated the hfs of several atomic spectra optically, and showed that  $\sigma_d$  for different elements is indeed different from the value previously accepted; and, furthermore, that  $\sigma_d$  shows a tendency to increase with increasing atomic number,  $Z$ . He concluded that for Lu,  $\sigma_d = 20$  should be a better approximation.

In his derivation, Murakawa used the value  $\mu_I(\text{Lu}^{175}) = 2.77$  nm, which he had determined by means of the Fermi-Segré formula from the  $A(s)$  factor for the  $5d6s$   ${}^2D$

<sup>39</sup> K. Murakawa, Phys. Rev. **98**, 1285 (1955).

term, as measured by Gollnow.<sup>3</sup> Steudel<sup>4</sup> obtained the same  $A(s)$  factor as Gollnow, but arrived at a value for  $\mu_I$  which is drastically different from Murakawa's—viz., 2.0 nm. Hence, an attempt was made to check Murakawa's conclusions concerning  $\sigma_d$  by calculating the screening corrections for the  $d$  electrons in the  $nd(n+1)s^2$  ground-state configurations of the group III elements. The published atomic beam data on the ground-state hfs of Sc,<sup>35</sup> Y,<sup>34</sup> and La<sup>8</sup> (the  $A$  factors being corrected for configuration mixing by the method of Sec. III) combined with the values for the magnetic moments of these nuclei, obtained from NMR measurements,<sup>40–43</sup> were used in Eqs. (2a) and (2c). We assume, for the moment, ignorance of the NMR value of  $\mu_I$  for lutetium. The  $Z_i$  values calculated in this way are given in Table VII together with some values given by Murakawa. As can be seen, the value for La agrees very well with that of Murakawa.

When the  $Z_i$  values for the first three elements are plotted against atomic number  $Z$ , a linear relationship seems to result from which, by extrapolation, the value  $Z_i=Z-19.5=51.5$  is obtained for Lu. In the last line

 TABLE VII. Screening corrections for  $d$  electrons.

Element	Electron	$Z$	$\sigma_d$	$Z_i$	
				Derived as in text	Murakawa
Sc	3 <i>d</i>	21	12	9	
Y	4 <i>d</i>	39	14.5	24.5	
La	5 <i>d</i>	57	17.5	39.5	39.7
Lu	5 <i>d</i>	71	19.5	51.5	51.0

of the table, Murakawa's value is compared with this extrapolated value. The good agreement between these values is most interesting, since on the one hand Murakawa's value is based on an incorrect value for the magnetic moment and on the other hand, the extrapolation procedure used here may have no theoretical justification. The reliability of this value is difficult to assess. Grave doubts are cast on it when it is used to calculate the nuclear magnetic moment from the interaction constants, as shown in the next paragraph.

### (b) Nuclear Magnetic Dipole Moment from the $A$ Factors

Assuming  $Z_i=51.5$  and using values of  $A'$  and  $A''$  corrected for configuration interaction in the manner described in Sec. V(c) we find, through Eqs. (2a) and (2c), the value  $\mu_I(\text{corrected})=2.0178$  nm. This agrees with the value  $\mu_I=2.0$  nm obtained by Steudel<sup>4</sup> from

<sup>40</sup> D. M. Hunter, Phys. Rev. **78**, 806 (1950).

<sup>41</sup> E. Brun, J. Oeser, E. E. Staub, and C. G. Telschow, Phys. Rev. **93**, 172 (1954).

<sup>42</sup> W. C. Dickenson, Phys. Rev. **76**, 1414 (1949).

<sup>43</sup> R. E. Sherriff and D. Williams, Phys. Rev. **82**, 651 (1951).

 TABLE VIII. Experimental  $Q$  values obtained from the  ${}^2D_{3/2}$  and  ${}^2D_{5/2}$  data.

State	$Q$ in $10^{-24}$ cm <sup>2</sup>
${}^2D_{3/2}$	5.74
${}^2D_{5/2}$	5.63

the  $A(s)$  factor of the  $5d6s\ {}^3D$  term of LuII but it disagrees with the correct value of 2.229nm. This disagreement may arise from the value of  $Z_i$  used, or from the procedure for correcting the observed  $A$ 's for configuration interaction, or even from the relativistic correction factors. If we assume, however, that the disagreement arises entirely from an incorrect  $Z_i$ , then the value which removes this disagreement is  $Z_i=57.8=Z-13.2$ . This means that the extrapolation procedure used above is not valid.

For the evaluation of the nuclear electric quadrupole moment we shall use  $Z_i=57.8$ .

### (c) Nuclear Electric Quadrupole Moment

The Eqs. (2a), (2b), and (2c) may be combined to give expressions for  $Q$  either in terms of  $B/\delta$ , or in terms of  $B/A_0$ . From (2b) and (2c), we have

$$Q = (B/\delta)Z_i \left[ 2.911a_0^3 \frac{h \times 10^6}{e^2} \right] \times (2L+1) \left( \frac{2J+2}{2J-1} \right) (H/R); \quad (4a)$$

and from (2a) and (2b), we have

$$Q = (B/A_0)(F/R) \left( \frac{g_I' \mu_0^2}{e^2} \right) \left( \frac{2J+2}{2J-1} \right) \left[ \frac{2L(L+1)}{J(J+1)} \right]. \quad (4b)$$

Because of the interrelation between  $A_0$ ,  $Z_i$ , and  $g_I'$ , these two expressions are equivalent and lead to the values of  $Q$  shown in Table VIII. No corrections for configuration interaction have been made for  $B$ . The difference between the two values obtained for different  $J$  is a direct consequence of the deviation of  $B''/B'$  from the theoretically expected ratio. The mean of these values<sup>44</sup> is

$$Q = +(5.68 \pm 0.06) \times 10^{-24} \text{ cm}^2.$$

Steudel,<sup>4</sup> using his optical data on the  ${}^2D$  and  ${}^3D$  terms uncorrected for configuration mixing, with  $Z_i=Z-11$ , obtained the value  $Q = +(5.6 \pm 0.6) \times 10^{-24}$  cm<sup>2</sup>, while Kamei<sup>45</sup> using Gollnow's<sup>3</sup> data for the  ${}^2D_{3/2}$  state with  $Z_i=Z-20$ ,<sup>39</sup> suggests  $Q = +(5.15 \pm 0.3) \times 10^{-24}$  cm<sup>2</sup>.

<sup>44</sup> Here the Sternheimer correction for induced quadrupole moment [Phys. Rev. **80**, 102 (1950); **84**, 244 (1951); **86**, 316 (1952); **95**, 736 (1954); **105**, 158 (1957)] has not been applied.

<sup>45</sup> I. Kamei, Phys. Rev. **99**, 789 (1955).

## VII. CONCLUSION

It has been shown that the observed hfs of Lu<sup>175</sup> can be understood in terms of current hfs theory provided one assumes that the 5*d*6*s*<sup>2</sup> ground configuration contains an admixture of higher configurations. The magnetic dipole and electric quadrupole moments of the Lu nucleus have been computed. Lack of knowledge of the exact wave functions of the ground state introduces uncertainties, however. More theoretical work seems necessary for a complete understanding of the experimental observations.

## ACKNOWLEDGMENTS

The author gratefully acknowledges the award of a National Research Council Postdoctorate Fellowship. He wishes to thank particularly Dr. Hin Lew for continued assistance, advice, and encouragement in the experiments described above; also, Dr. G. Herzberg, Dr. A. E. Douglas and the other members of this Laboratory for their keen interest. He is also indebted to Dr. Howard A. Shugart of the University of California, Berkeley, for his interest and suggestions, and for the computer processing of the data.

## Nuclear Spin, Hyperfine Structure, and Nuclear Moments of 6.8-Day Lutetium-177†

F. RUSSELL PETERSEN\* AND HOWARD A. SHUGART

*Department of Physics and Lawrence Radiation Laboratory, University of California, Berkeley, California*

(Received November 6, 1961)

The atomic-beam magnetic-resonance method has been used to measure the nuclear spin and hyperfine structure of 6.8-day Lu<sup>177</sup> in the ground <sup>2</sup>D<sub>3/2</sub> state and in the <sup>2</sup>D<sub>3/2</sub> electronic state. The results are:  $I = \frac{7}{2}$ ; <sup>2</sup>D<sub>3/2</sub>:  $a = 194.84(2)$  Mc/sec,  $b = 1466.71(12)$  Mc/sec; <sup>2</sup>D<sub>5/2</sub>:  $a = 147.17(1)$  Mc/sec,  $b = 1805.93(14)$  Mc/sec. The uncorrected nuclear moments for Lu<sup>177</sup> calculated from these measurements and from known constants of Lu<sup>175</sup> are:  $\mu_I = +2.217(10)$  nm,  $Q = +5.51(6)$  b.

## I. INTRODUCTION

AN atomic-beam magnetic-resonance study of the ground-state nuclear properties of radioactive lutetium isotopes has started with reactor-produced Lu<sup>177</sup>.<sup>1</sup> This isotope was a reasonable choice since it could be produced easily in metallic form from stable lutetium metal by the (*n*, $\gamma$ ) reaction and would likely possess properties similar to those of stable Lu<sup>175</sup> described in the preceding paper by Ritter.<sup>2</sup> A systematic knowledge of the spins and static moments in this highly deformed region of nuclides should furnish valuable test information for nuclear theories of the ground state as well as provide a basis for nuclear spectroscopic studies.

## II. THEORY OF THE EXPERIMENT

The atomic beam technique provides a sensitive method for observing radio-frequency transitions between two energy states of a free atom whose

Hamiltonian is

$$\begin{aligned} \mathcal{H}(\text{Mc/sec}) = & a\mathbf{I} \cdot \mathbf{J} + b[3(\mathbf{I} \cdot \mathbf{J})^2 + \frac{3}{2}(\mathbf{I} \cdot \mathbf{J}) \\ & - I(I+1)J(J+1)]/2I(2I-1)J(2J-1) \\ & - g_I(\mu_0/h)\mathbf{I} \cdot \mathbf{H} - g_J(\mu_0/h)\mathbf{J} \cdot \mathbf{H}, \quad (1) \end{aligned}$$

where  $\mathbf{I}$  and  $\mathbf{J}$  are the nuclear and electronic angular momenta in units of  $\hbar$ ,  $a$  and  $b$  are the dipole and quadrupole hyperfine-structure coupling constants,  $\mathbf{H}$  is the applied external magnetic field, and  $g_I$  and  $g_J$  are the nuclear and electric  $g$  factors defined by  $\mu_I/I$  and  $\mu_J/J$ , respectively, where the magnetic moments  $\mu_I$  and  $\mu_J$  are in units of the Bohr magneton  $\mu_0$ . The terms in this Hamiltonian are, from left to right: the magnetic dipole interaction between the nuclear magnetic moment and the electronic magnetic field; the electric quadrupole interaction between the nuclear electric quadrupole moment and the gradient of the electric field produced by the electrons; the interaction between the nuclear magnetic moment and the applied external field; and the interaction between the electronic magnetic moment and the applied external field.

The eigenvalues of this Hamiltonian may be found by using digital computing techniques, and hence the energy levels may be obtained as a function of the various parameters in Eq. (1). Figures 1 and 2 show some of the levels in the <sup>2</sup>D<sub>3/2</sub> and <sup>2</sup>D<sub>5/2</sub> states of Lu<sup>177</sup> as a function of the external magnetic field. Primarily those

† This research is supported in part by the U. S. Air Force Office of Scientific Research and the U. S. Atomic Energy Commission.

\* Now at the National Bureau of Standards, Boulder Laboratories, Boulder, Colorado.

<sup>1</sup> F. R. Petersen and H. A. Shugart, *Bull. Am. Phys. Soc.* **5**, 273 (1960); **6**, 224 (1961).

<sup>2</sup> George J. Ritter, preceding paper [*Phys. Rev.* **125**, 240 (1962)].